DESIGN AND IMPLEMENTATION OF A VISUAL MONITORING SYSTEM FOR PADDY FLOW INSTABILITY IN INTELLIGENT HUSKERS

/

面向智能砻谷机的稻谷料流失稳视觉监测系统设计与实现

Min CHENG *1), Shihao ZHOU1), Yong PAN2), Xingchuang WANG1)

1) School of Mechanical and Electrical Engineering, Henan University of Technology, Zhengzhou / China;

2) School of Intelligent Engineering, Henan Mechanical and Electrical Vocational College, Zhengzhou / China

Corresponding author: Min Cheng, Tel: +86-18623710936; E-mail: chengminhappy2006@163.com,

DOI: https://doi.org/10.35633/inmateh-79-19

Keywords: *Rubber roll husker; Paddy flow; Machine Vision; Real-time monitoring*

ABSTRACT

To achieve precise prevention and control of rubber roll wear in huskers, this study established a complete experimental platform integrating mechanical transmission, feeding control, and visual acquisition units, and subsequently developed a real-time monitoring system for paddy flow instability based on machine vision. An image acquisition system composed of a CMOS camera and a customized light source was built to construct a dedicated dataset for paddy flow states. Based on the lightweight YOLOv8n detection model, Python programming was adopted in the PyCharm environment with the Ultralytics library integrated, realizing real-time recognition and quantitative analysis of paddy flow states. The results demonstrated that the system realized a real-time detection efficiency of 14 FPS on a local workstation, and the YOLOv8n model achieved a recognition accuracy of 90.8% in terms of mean Average Precision at IoU threshold 0.5 (mAP@0.5) for sparse and overlapping grain states. The system could effectively capture key abnormal states, including inclined paddy grains entering the rolling zone, sparse paddy flow lasting more than 5 seconds, and overlapping paddy flow density exceeding 10 grains/cm². This study transformed the mechanical characteristics of paddy flow instability into pixel-level quantitative indicators and established an integrated visual monitoring paradigm of "perception-analysis-decision", providing effective technical support for the intelligent management and control of huskers.

摘要

为实现砻谷机胶辊磨损的精准防控，本研究搭建了集成机械传动、喂料控制与视觉采集单元的完整实验平台，开发了基于机器视觉的稻谷料流失稳实时监测系统。采用 CMOS 相机与定制光源构建图像采集系统，构建稻谷料流状态专用数据集；基于 YOLOv8n 轻量化检测模型，在 PyCharm 环境中采用 Python 编程集成 ultralytics 库，实现料流状态的实时识别与量化解析。结果表明，该系统在本地工作站可实现 14FPS 的实时检测效率，YOLOv8n 模型对颗粒稀疏与堆叠状态的识别精度（交并比 0.5 阈值下的平均精度均值，mAP@0.5）达到 90.8%，可有效捕捉稻谷颗粒入轧倾斜、料流稀疏持续时间大于 5 秒、料流堆叠密度超过 10 粒/cm²等关键异常状态。本研究将料流失稳的力学特征转化为像素级量化指标，构建"感知-解析-决策"一体化视觉监测范式，为砻谷机智能管控提供了有效的技术支撑。

INTRODUCTION

During the operation of a rubber roll husker, the uniform wear condition of rubber rolls is crucial for maintaining a stable hulling process (*Prabhakaran et al., 2017*). Studies indicate that the dynamic imbalance in paddy flow distribution is the fundamental cause of uneven rubber roll wear (*Yehia & Katab, 2018*). However, constrained by the complex environment of the rolling zone, existing industrial sensors struggle to accurately monitor dynamic paddy flow conditions. To address this, there is an urgent need to develop a machine vision-based monitoring system. By enabling online recognition and analysis of the paddy flow before it enters the rolling zone, the system can accurately capture unstable flow patterns and provide real-time data support for subsequent control. The technology enables the prevention of rubber roll wear from the source and offers a new paradigm for the intelligent upgrading of grain processing equipment.

Early monitoring technologies primarily focused on mechanical parameters. For instance, Zhancheng Grain Machinery Factory in Zhejiang developed a real-time roll pressure monitoring system that uses sensors to provide immediate feedback on pressure data, offering visual guidance for manual operation (*Xiang and Ruan, 2009; Zhou et al., 2025*).

Wang et al. (2013) introduced a PLC control system into the rubber roll husker, integrating functions such as equipment start-stop, flow regulation, and fault alarm, thereby preliminarily achieving automated management of the hulling process. *Wang (2016)* designed a real-time monitoring system that breaks through single-dimensional limitations by simultaneously collecting parameters such as rubber roll speed, roll pressure, and flow rate, enabling intelligent management of operational parameters. Furthermore, uneven feeding during rubber roll husker operation leads to uneven wear of the rubber rolls, which can cause vibration and noise. *Wu et al. (2024)* conducted real-time detection and identification of abnormal wear conditions on the rubber rollers of a husker based on point cloud data, effectively addressing the challenge of accurately monitoring the wear state of rubber rollers. *Zhu (1979)* pointed out that rubber roll eccentricity is caused by vibration during the hulling process. To address this issue, *Liu (2020)* applied a multi-link vibration isolation concept within the rolls and designed an impact isolator, which mitigated shock vibration transmission and acoustic radiation in the rubber roll husker. Future studies should further investigate the influence of uneven rubber roll wear on rotor dynamic characteristics to mitigate vibration and noise.

In the field of material flow monitoring, although existing bulk material monitoring technologies are quite diverse, specialized research on paddy flow remains scarce. Current achievements mainly focus on belt conveyor scenarios in industries such as coal, while the physical and chemical characteristics of paddy differ significantly from other materials, imposing higher requirements on monitoring technology. For material flow monitoring on belt conveyors, *Wen et al. (2023),* integrated line laser and binocular vision techniques to detect coal flow on the conveyor belt, and achieved high-precision volumetric flow calculation through host computer processing. The method exhibits limited adaptability to complex conditions in paddy flow, such as overlapping and inclination. *Xu et al. (2022)* integrated RFID technology with point cloud data processing methods to achieve real-time measurement of the mass flow rate of bulk materials on a conveyor belt, obtaining high-precision results on fine sand materials, which can provide a reference for similar applications in paddy flow monitoring. *Yan et al. (2023)* employed a dual-array capacitive sensor combined with the BP-Adaboost algorithm to realize multi-parameter measurement of gas–solid two-phase flow, effectively improving the identification capability for complex flow conditions such as sparse or stacked particles. *Zhu et al. (2024)* evaluated the measurement performance of an array capacitive sensor for particle concentration in gas–solid two-phase flow through a CFD-DEM coupling method, thereby laying a theoretical foundation for precise monitoring of particle flow. However, this method requires adaptive optimization for the specific characteristics of paddy flow to enhance the accuracy and stability of the monitoring system.

Current paddy flow monitoring faces three challenges: the difficulty in balancing accuracy with adaptability, the insufficient reliability of low-cost sensors, and the disconnection between monitoring and control processes. Therefore, this paper proposes an integrated visual monitoring paradigm of "perception-analysis-decision". By converting the mechanical characteristics of paddy flow instability into pixel-level quantitative indicators, it establishes a closed-loop feedback channel for the full-cycle intelligent management of rubber rolls.

MATERIALS AND METHODS

The feeding device and the visual acquisition unit form the hardware core of the system, working in coordination with the host computer to establish a comprehensive paddy flow status monitoring framework.

Mechanical system structure and functional implementation

The structure and control performance of the feeding device directly determine the data reliability of the monitoring system. This apparatus adopts a combined long and short chute board structure and employs modular design to achieve precise simulation and regulation of paddy flow conditions. As shown in Fig. 1(a), the device consists of a hopper, feeding roller, electric motor, long and short chute boards, chute adjustment mechanism, and support frame.

The electric motor drives the feeding roller at a constant speed, ensuring continuous and stable material conveyance. The long and short chute boards facilitate uniform material distribution and guided flow through their uniquely designed inclination angles. The integrated Q312B leaf spring nut and butterfly bolt assembly enables stepless adjustment of the chute inclination, thereby allowing precise control over paddy flow velocity and density distribution. The support frame employs a rigid connection design to effectively suppress mechanical vibration interference with the paddy flow state. Through coordinated mechatronic control, the entire setup provides stable and reliable experimental conditions for the visual monitoring system.

Software architecture and data processing flow

The vision acquisition system establishes a comprehensive technical framework for paddy flow monitoring through the integration of hardware and software algorithms. As shown in Fig. 1(b), the vision acquisition unit adopts a modular design incorporating a Hikvision MV-CU013-A0UC CMOS industrial camera, MVL-HF0628M-6MPE 6mm fixed-focus lens, and ring LED light source (*Yu, 2024*).

The system utilizes a C-mount interface and USB 3.0 protocol to establish a high-speed data transmission channel. The camera ensures complete capture of dynamic paddy flow characteristics through its high-frame-rate acquisition capability. The lens maintains geometric imaging accuracy with a low distortion rate of -0.103%. The ring light source effectively suppresses localized shadows and enhances grain texture features through multi-angle uniform illumination. Under the centralized management of MVS V4.4.0 professional software, the unit achieves unified control of parameters including acquisition frequency, resolution, and image format. All hardware components operate in coordination with the computer-based main control system through standard communication protocols, collectively forming a stable and reliable visual perception foundation. Feeding device with combined long and short chute boards (*Zhang et al., 2024*).

The system software employs a multi-threaded architecture developed in a Python-OpenCV environment, implementing three core functional modules. The image acquisition module captures 640×640 resolution video streams at 168 FPS through the VideoCapture interface, performing color space conversion and image preprocessing. The model inference module utilizes the Ultralytics library to load an optimized YOLOv8 model, executing object detection with preset confidence and IoU thresholds to output particle localization and classification data. The visualization module integrates functions for rendering detection bounding boxes, annotating categories, and counting particles, supporting real-time display and result storage. Each module exchanges data through asynchronous message queues, working in conjunction with MVS professional software to manage device control and parameter configuration, thereby establishing a complete "acquisition-analysis-display" processing pipeline. By integrating the computer, image acquisition module, and feeding device, an efficient and stable image acquisition platform was established. The structural model diagram of this platform is shown in Fig. 2, providing a foundation for subsequent object detection and analysis.

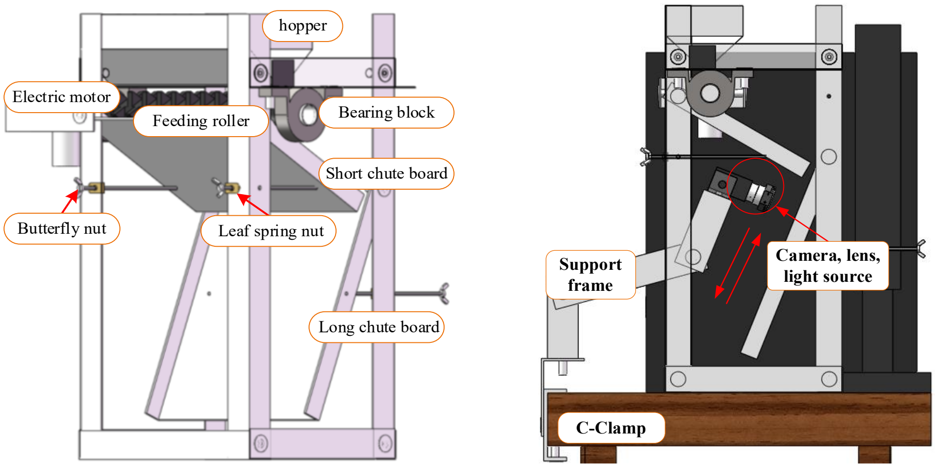

(a) Schematic diagram of feeding device (b) Diagram of camera mount position adjustment

Fig. 1 - Paddy flow monitoring system

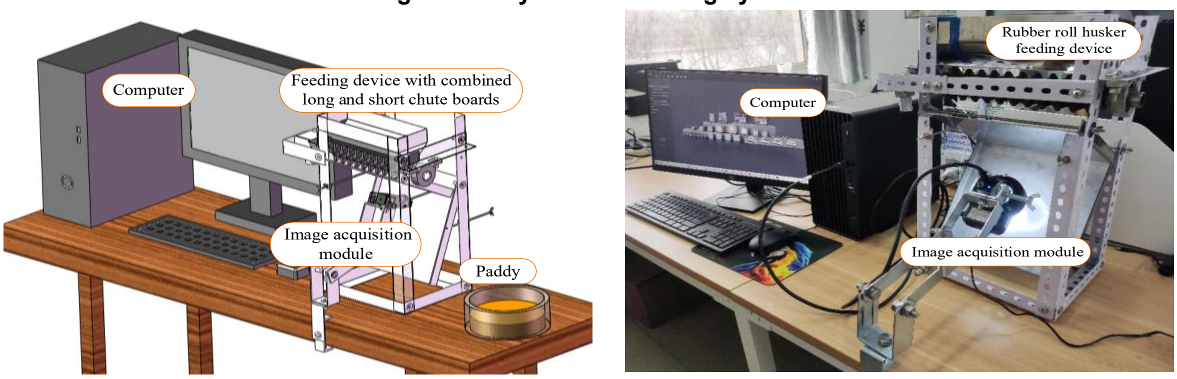

(a) Design diagram of the visual monitoring platform (b) Physical photograph of the visual monitoring platform

Fig. 2 - 3D structural design and physical experimental platform for the flow monitoring system

Paddy flow dataset construction

YOLOv8 is an object detection algorithm based on convolutional neural networks. Building upon the YOLO series, it enhances detection performance by incorporating novel features and architectural improvements (*Ma et al., 2024; Paul et al., 2024; Tian., 2024*). The algorithm requires a large volume of image data with corresponding annotations as training samples. Through learning from these samples, it extracts features such as shape and color of paddy, thereby establishing a mapping relationship between input images and target detection results. To accurately identify paddy flow conditions, this study constructed a dedicated image dataset *(Ma et al., 2024)*. The dataset comprises a total of 530 images, including 220 static scenes and 310 dynamic scenes, divided into training and validation sets in an 8:2 ratio. Due to limitations in dataset size and annotation cost, only a training set and a validation set have been currently divided, with no separate test set established. Model performance evaluation is primarily conducted based on the validation set, while the model's generalization capability is further verified through dynamic real-time monitoring experiments. Future work will expand the dataset and introduce an independent test set to refine the evaluation framework. Using the LabelImg tool, manual annotations were performed in YOLO format, generating label files containing target bounding box coordinates and category labels. During annotation, sparse and overlapping paddy flow conditions were labeled as Sparse Grains (SG) and Pile-up Scenes (PS) tags respectively (*Song, 2025*). As shown in Fig. 3, for sparsely distributed grains, each grain was individually annotated with SG tags; for overlapping regions, whether single-layer or multi-layer distribution, they were uniformly labeled as PS tags to ensure the model can effectively learn morphological features of grains under different density conditions.

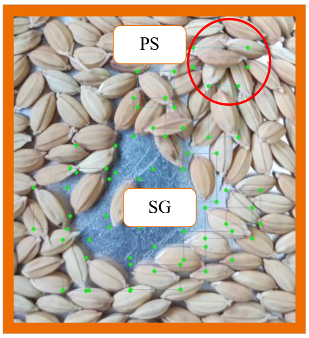

Fig. 3 - Labeling of paddy condition data

Model training via comparative experiments

During the model training phase, the YOLOv8 training parameters were configured within the PyCharm development environment. The yolov8n.pt, yolov8s.pt, and yolov8m.pt pre-trained models were selected for a comparative experiment to evaluate their performance on the paddy flow dataset. For data configuration, the dataset path was explicitly specified via a configuration file, with "SG" and "PS" defined as the two target categories. In the hyperparameter settings, the number of training epochs was set to 100, the batch size was set to 4, the initial learning rate (lr0) was 0.01, and the final learning rate (lrf) was 0.01, using a cosine annealing scheduling strategy. All models were trained under identical experimental settings to ensure comparability of the results (*Ma, 2021*). The complete algorithm workflow is shown in Fig. 4.

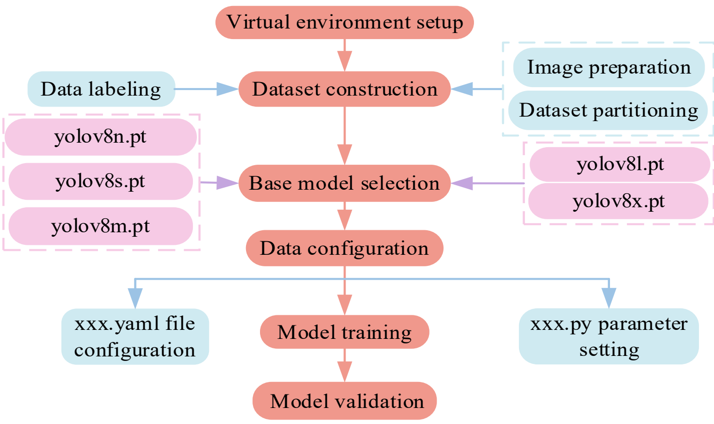

Fig. 4 - YOLOv8 application flowchart

RESULTS

Comprehensive model performance evaluation

Based on the YOLOv8 architecture, a comparative experiment was conducted using three model specifications named yolov8n.pt, yolov8s.pt and yolov8m.pt on a self-built paddy flow dataset. Through comprehensive evaluation using metrics including mAP@0.5, FPS and model size, the most suitable model architecture for dynamic monitoring scenarios was successfully identified (*Ma et al., 2025*).

Table 1

Performance metrics of different model specifications on the paddy flow dataset

Method	mAP0.5(%)	mAP0.5:0.95(%)	Frame Rate (FPS)	Model Size(MB)
YOLOv8n	90.8	73.1	14	6.3
YOLOv8s	89.5	74.2	9	22.5
YOLOv8m	92.4	77.2	3	52

Experimental results demonstrate notable performance disparities among the YOLOv8 series models in paddy flow detection tasks. As shown in Table 1, the nano model YOLOv8n achieves the optimal balance between accuracy and speed, attaining 90.8% mAP@0.5 with a compact model size of 6.3MB and an inference speed of 14 FPS. This demonstrates its strong capability in identifying sparse paddy flow conditions, making it suitable for deployment in computationally constrained small-scale rubber roll huskers. However, its mAP@0.5:0.95 of 73.1% falls below that of the medium model, indicating insufficient precision in target localization at lower IoU thresholds. The small model YOLOv8s shows suboptimal performance in both detection accuracy (89.5%) and processing speed (9 FPS), primarily attributable to increased network depth causing loss of shallow features. In contrast, YOLOv8m demonstrates comprehensive leadership in detection accuracy, achieving 92.4% mAP@0.5 and 77.2% mAP@0.5:0.95. Its deep feature pyramid effectively integrates multi-scale information, successfully addressing occlusion problems caused by paddy flow accumulation. Nevertheless, its practical application remains constrained by an inference speed of 3 FPS and a substantial model size of 52MB. Additionally, setting the training batch size to 4 may theoretically have a slight impact on model generalization performance. As shown in Table 1, all three models completed effective training in the paddy flow detection task, yielding stable and reliable detection results. The core focus of this study is to verify the monitoring feasibility of lightweight models, and the negative impact of this parameter setting on the final detection performance is within an acceptable range.

Table 2

Comparative analysis of performance metrics for different model variants on the paddy flow dataset

Parameter	YOLOv8n	YOLOv8s	YOLOv8m
Detection accuracy	Strong in sparse scenes Weak in overlapping scenes	Lowest overall performance	Optimal for all scenarios
Inference speed	14 FPS (Excellent real-time performance)	9 FPS (Suboptimal efficiency)	3 FPS (Severe delay)
Hardware compatibility	Embedded device friendly	Cost-ineffective	Requires GPU server support
Data dependency	Sensitive to low-resolution input	Sensitive to feature distribution	Requires high-quality training data

As shown in Table 2, comparative analysis of performance metrics from different model specifications on the paddy flow dataset demonstrates that although YOLOv8m achieves optimal detection accuracy, the final selection was determined to be YOLOv8n as the core model for paddy flow monitoring, considering the system's stringent requirements for real-time performance and embedded deployment. This model achieves the best balance between accuracy and speed, with its compact 6.3MB size and 14 FPS inference speed better aligning with practical engineering applications, thereby establishing a reliable technical foundation for real-time monitoring of paddy flow states in rubber roll huskers.

Evaluation of model prediction results

During the training of the YOLOv8 model, the convergence curve serves as a critical indicator for evaluating training effectiveness.

As shown in Fig. 5(a), the YOLOv8n model demonstrates favorable convergence characteristics on the paddy flow dataset. The bounding box regression loss decreases from 1.2 to 0.6, while the classification loss on the validation set exceeds that of the training set by 0.1, suggesting mild overfitting. Fluctuations in the object confidence loss within the validation set indicate that the model's adaptability to complex scenarios requires further improvement. Performance metrics reveal a precision of 0.8 and a recall of 0.75, with mAP50 reaching 0.82.

However, mAP50-95 plateaus at 0.68, indicating a performance bottleneck in detection under high IoU thresholds. After 50 training epochs, the model stabilizes, with the performance gap between the training and validation sets controlled within 5%, demonstrating robust generalization capability.

Analysis of convergence curves for YOLOv8s and YOLOv8m on the paddy flow dataset reveals distinct training patterns. YOLOv8s shows a decrease in bounding box loss from 1.2 to 0.6, with the validation set converging at 0.8, demonstrating progressive improvement in localization capability. However, the model displays noticeable overfitting as evidenced by a validation classification loss of 1.0 significantly exceeding the training loss of 0.5. Additionally, fluctuations in objectness loss reaching 1.2 on the validation set indicate limited generalization capability. The performance metrics show precision and recall values of 0.8 and 0.7, respectively, on the validation set, with mAP50 reaching 0.8, while mAP50–95 plateaus at 0.6 and shows slower growth.

Similarly, YOLOv8m exhibits a decline in bounding box regression loss from 1.2 to 0.6 in training and 0.8 in validation, confirming continuous localization improvement. Nevertheless, the model demonstrates pronounced overfitting with a validation classification loss of 1.0 compared to the training loss of 0.5. Objectness loss fluctuations up to 1.2 in validation further reveal inadequate generalization capacity. Performance metrics indicate validation precision of 0.8, recall of 0.7, and mAP50 of 0.8, while mAP50-95 stabilizes at 0.6 with decelerated growth. Both architectures consequently face limitations in high-threshold detection performance despite their steady progress in localization accuracy.

Convergence curve analysis reveals that YOLOv8s exhibits elevated validation loss with overfitting tendencies, while YOLOv8m demonstrates rapid initial convergence but subsequent instability. In contrast, YOLOv8n delivers optimal performance on the paddy flow dataset, characterized by synchronized and stable decline in both training and validation losses, demonstrating superior generalization capability that best aligns with the requirements of this monitoring task.

Classification accuracy is regarded as a vital metric for evaluating the classification capability of YOLOv8 models. When a model maintains high accuracy on both training and validation sets, it indicates effective fitting while possessing strong generalization capability. As shown in Fig. 5(b), the confusion matrix analysis of YOLOv8n demonstrates 78% recognition accuracy for overlapping paddy flow and 70% accuracy for sparse paddy flow, with cross-misclassification rates between both categories remaining below 3%. However, the background misclassification rates reach 20% for overlapping flow and 29% for sparse paddy flow, indicating the current model's capability to distinguish complex backgrounds requires further enhancement.

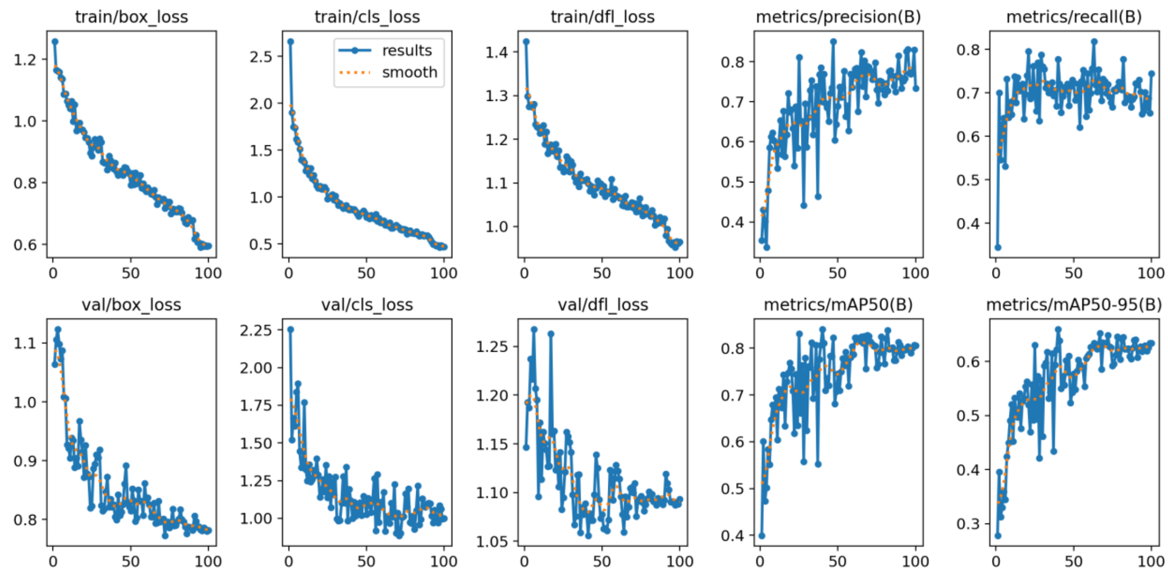

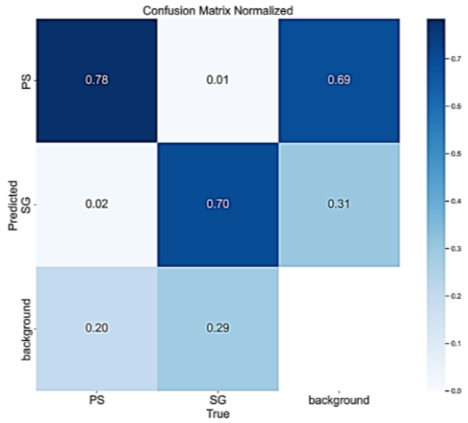

(a) Convergence curve of Yolov8n on the paddy flow dataset (b) Confusion matrix of YOLOv8n

Fig. 5 - Training dynamics and classification performance of YOLOv8n

Confusion matrix analysis of YOLOv8s indicates 65% recognition accuracy for overlapping paddy flow and 68% for sparse conditions, with a cross-misclassification rate of merely 2% between these two categories. However, the background misclassification rates reach critically high levels of 34% and 32% respectively, suggesting inadequate learning of background features and heightened susceptibility to interference from target characteristics. For YOLOv8m, the recognition accuracy for SG reaches 86%, while its predictive accuracy for PS remains notably low at 55%, demonstrating strong SG identification capability but significant errors in PS detection. The absence of cross-misclassification between categories confirms high accuracy in single-target recognition. Additionally, PS and SG instances are misclassified as background at substantial rates of 45% and 14% respectively, indicating prevalent background misclassification issues.

Classification accuracy analysis demonstrates that YOLOv8n achieves optimal overall performance in paddy flow detection, with recognition accuracies of 78% for overlapping paddy flow and 70% for sparse paddy flow, while maintaining cross-misclassification rates below 3% between categories. Despite background misclassification rates ranging from 20% to 29%, it still exhibits superior performance compared to other models. Both YOLOv8m and YOLOv8s exhibit specific limitations, either in particular scenario recognition capabilities or overall performance deficiency, accompanied by notably high background misclassification rates. Comprehensive evaluation confirms YOLOv8n as the preferred solution for achieving simultaneous accurate identification of both sparse and overlapping states in paddy flow.

Validation of the paddy flow monitoring system

To verify the practical performance of the material flow monitoring system, this study conducted system validation based on a dynamic material flow simulation platform in a local workstation environment equipped with a 12th-generation Intel Core i7 processor, 32 GB of RAM, and no GPU acceleration. A graded quantitative characterization system was proposed to systematically describe sparse and overlapping unstable states of paddy flow by defining grain density levels within a unit area. For sparse paddy flow conditions, three severity levels were established based on grain count per unit area: mild (10~20 grains), moderate (25~40 grains), and severe (45~60 grains). For overlapping paddy flow conditions, both single-layer and multi-layer structures were uniformly annotated as overlapping regions using the same grain quantity classification criteria. The system implements dynamic visualization of detection results through Python programming, enabling real-time display of distributed sparse and overlapping paddy flow regions at different severity levels.

The system achieves deep integration with the CMOS camera SDK through Python-OpenCV. Within the PyCharm development environment, it utilizes the Ultralytics library to load the trained YOLOv8n model weights and employs a multi-threaded architecture for synchronous processing of image acquisition and model inference tasks. For the dynamic and non-stationary monitoring scenario of paddy flow, the system must achieve real-time image sensing, instant processing, and fast inference. It should synchronously perform acquisition, detection, and recognition during transient changes in the flow state, ensuring high synchronization between the output results and the actual flow state, thereby meeting the timeliness and real-time decision-making requirements of online dynamic material flow monitoring (*He et al., 2025*). The system achieves real-time monitoring of dynamic paddy flow parameters via an asynchronous message queue mechanism, stably outputting key state information such as sparse and overlapping grain distributions. The real-time monitoring performance is illustrated in Fig. 6.

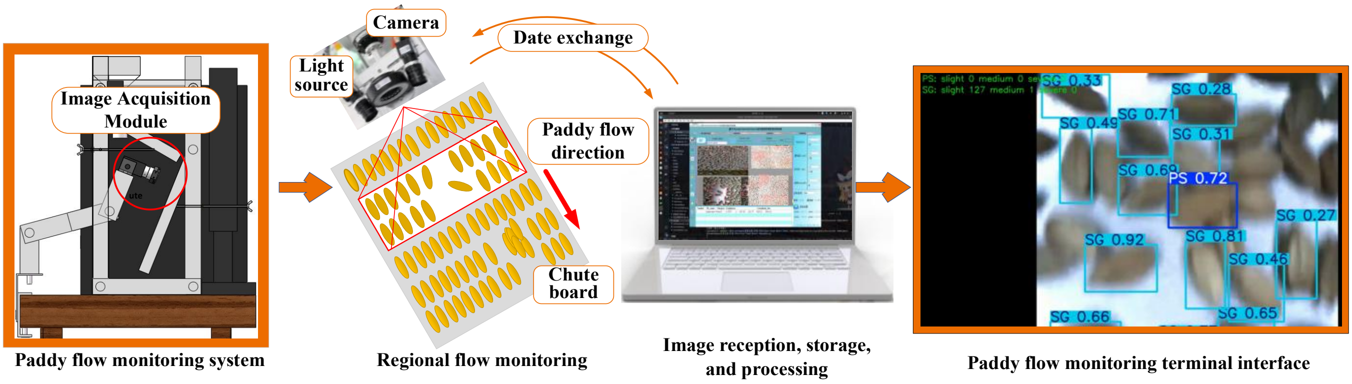

Fig. 6 - Real-time monitoring of sparse and overlapping paddy flow

Validation results demonstrate that the system maintains a stable frame rate of 14 FPS when processing 640×640 resolution video streams, meeting the real-time monitoring requirements. *Chen et al. (2020)* developed a real-time vision-based detection system for dynamic grain flow monitoring in rice combine harvesters and showed that a frame rate of 10~20 FPS is sufficient to capture transient changes in agricultural material flow and fulfill the engineering requirements for online detection. The comprehensive recognition accuracy for sparse and overlapping paddy flow states reaches 89.7%, enabling synchronous output of critical information including sparse and overlapping paddy flow conditions. The asynchronous message queue mechanism ensures stable data exchange, with memory usage remaining stable at approximately 1.8 GB during testing. The system demonstrates excellent engineering applicability and robustness, providing effective technical support for intelligent control of rubber roll huskers.

CONCLUSIONS

Addressing the issue of uneven wear in rubber roll huskers caused by unstable paddy flow, this paper systematically investigates machine vision-based monitoring methods for paddy flow conditions.

By constructing a dedicated image dataset, developing an optimized lightweight detection model, and integrating hardware-software systems, the feasibility and effectiveness of this technical approach in engineering applications have been verified.

The main conclusions are as follows:

(1) A comprehensive technical solution for paddy flow status monitoring has been proposed. This solution systematically establishes a technical framework encompassing image acquisition platform construction, multi-scenario data collection, specialized dataset development, and monitoring system integration, providing a reusable methodological foundation for dynamic paddy flow monitoring.

(2) Comparative experiments based on the YOLOv8 architecture demonstrate that the YOLOv8n nano model achieves the best balance between accuracy and speed. Although its mAP@0.5 of 90.8% is lower than that of YOLOv8m, its inference speed and model size are superior to the latter, while maintaining a real-time processing speed of 14 FPS, thereby fully meeting the real-time requirements of the husker operation scenario.

(3) The real-time paddy flow monitoring system exhibits significant engineering application value. Through coordinated hardware-software design, the system accurately identifies unstable paddy flow conditions including sparse and overlapping states in dynamic paddy flow, providing effective technical support for wear control in rubber roll huskers.

This research validates the application potential of machine vision technology based on lightweight deep learning models in agricultural mechanization. The proposed monitoring solution not only offers a novel approach for quality control in rice processing but also serves as a technical reference for real-time monitoring of other agricultural materials. Future research may further explore the model's adaptability under more complex working conditions and its integration with data from other sensors.

ACKNOWLEDGEMENT

The authors acknowledge the financial support from Science and Technology Research Project of Henan (No.262102111069), the Joint Fund of Henan Provincial Science and Technology Research and Development Plan (No.232103810087), the R&D Special Fund Subsidy Research Project of Zhengzhou (No. 22ZZRDZX14).

REFERENCES

[1] Chen J., Lian Y., Zou R., Zhang S., Ning X., Han M. (2020). Real-time grain breakage sensing for rice combine harvesters using machine vision technology. *International journal of agricultural and biological engineering*, vol. 13, no. 3, pp. 194-199. DOI: https://doi.org/10.25165/j.ijabe.20201303.5478

[2] He X., Liu Z., Hu S., Liu C., Zhou D. (2025). Real-time safety assessment techniques of dynamic systems (动态系统的实时安全性评估技术). *Acta Automatica Sinica*, vol. 51, no. 2, pp. 249-270. DOI: https://doi.org/10.16383/j.aas.c240096

[3] Liu P. (2020). *Research on impact vibration isolation technology in rubber roll husking process (胶辊式砻谷的冲击振动隔离技术研究)*, MSc dissertation, Xihua University. DOI: https://doi.org/10.27411/d.cnki.gscgc.2020.000028

[4] Ma B., Hua Z., Wen Y., Deng H., Zhao Y., Pu L., Song H. (2024). Using an improved lightweight YOLOv8 model for real-time detection of multi-stage apple fruit in complex orchard environments. *Artificial Intelligence in Agriculture*, vol. 11, pp. 70-82. DOI: https://doi.org/10.1016/j.aiia.2024.02.001

[5] Ma F., Li S., Li J., Li Y., Duan L., Li L., Tan J., Wang Y. (2025). Millet ear detection method in UAV images based on improved YOLOx. *INMATEH-Agricultural Engineering*, vol. 75, no.1, pp.680-690. DOI: https://doi.org/10.35633/inmateh-75-59

[6] Ma N., Li Z., Kong Q. (2024). Wheat grains automatic counting based on lightweight YOLOv8. *INMATEH-Agricultural Engineering*, vol. 73, no.2, pp.592-602. DOI: https://doi.org/10.35633/inmateh-73-50

[7] Ma S. (2021). *Research and implementation of belt material flow detection algorithm based on machine vision (基于机器视觉的皮带料流检测算法研究与实现)*, MSc dissertation, Yanshan University. DOI: https://doi.org/10.27440/d.cnki.gysdu.2021.001282

[8] Paul A., Machavaram R., Kumar D., Nagar H. (2024). Smart solutions for capsicum Harvesting: Unleashing the power of YOLO for Detection, Segmentation, growth stage Classification, Counting, and real-time mobile identification. *Computers and Electronics in Agriculture*, vol. 219, pp. 108832. DOI: https://doi.org/10.1016/j.compag.2024.108832

[9] Prabhakaran P., Ranganathan R., Muthu Kumar V., Rajasekar R., Devakumar L., Pal S. (2017). Review on parameters influencing the rice breakage and rubber roll wear in sheller. *Archives of metallurgy and materials*, vol. 62, no. 3, pp. 1875-1880. DOI: https://doi.org/10.1515/amm-2017-0284

[10] Song J., Wu Z. (2025). Research on traffic sign detection based on YOLOv8n (基于 YOLOv8n 的交通标志检测研究). *Internet of Things Technologies*, vol. 15, no. 4, pp. 21-24+28. DOI: https://doi.org/10.16667/j.issn.2095-1302.2025.04.005

[11] Tian Y., Qin S., Yan Y., Wang J., Jiang F. (2024). Blueberry maturity detection in complex field environments based on improved YOLOv8 (基于改进 YOLOv8 的田间复杂环境下蓝莓成熟度检测). *Transactions of the Chinese Society of Agricultural Engineering*, vol. 40, no. 16, pp. 153-162. DOI: https://doi.org/10.11975/j.issn.1002-6819.202312044

[12] Wang H. (2016). *Design and research of automatic adjustment system for rubber roll husker (胶辊砻谷机自动调节系统的设计与研究),* MSc dissertation, Shanxi Agricultural University.

[13] Wang Y., Liu Y. (2013). Application of PLC automatic control technology in rice milling production lines (自动控制技术 PLC 在碾米生产线中的应用). *Heilongjiang Grain*, no. 5, pp. 55-56. DOI: https://doi.org/10.3969/j.issn.1671-6019.2013.05.025

[14] Wen L., Liang B., Zhang L., Hao B., Yang Z. (2023). Research on coal volume detection and energy-saving optimization intelligent control method of belt conveyor based on laser and binocular visual fusion. *IEEE Access*, vol. 12, pp. 75238-75248. DOI: https://doi.org/10.1109/ACCESS.2023.3261335

[15] Wu Z., Jin T., Liu X., Zhang Z., Zhao B., Zhang Y., He X. (2024). Research on the Wear State Detection and Identification Method of Huller Rollers Based on Point Cloud Data. *Coatings*, vol. 14, no. 9, pp. 1209. DOI: https://doi.org/10.3390/coatings14091209

[16] Xiang G., Ruan J. (2009). Current status and development overview of rubber roll huskers in domestic and international markets (国内外胶辊砻谷机现状及发展概述). *Grain Processing*, vol. 34, no. 5, pp. 60-65. DOI: https://doi.org/10.3969/j.issn.1007-6395.2009.05.019

[17] Xu S., Cheng G., Cui Z., Jin Z., Gu W. (2022). Measuring bulk material flow—Incorporating RFID and point cloud data processing. *Measurement*, vol. 200, pp. 111598. DOI: https://doi.org/10.1016/j.measurement.2022.111598

[18] Yan W., Yang D., Zhang Y., Li B. (2023). Twin-array capacitance sensor for multi-parameter measurement of gas-solid particle flow based on BP-Adaboost. *Flow Measurement and Instrumentation*, vol. 94, pp. 102445. DOI: https://doi.org/10.1016/j.flowmeasinst.2023.102445

[19] Yehia M.E., Katab A.R. (2018). Effect of hulling machines on hulling characteristics and quality of rice grains. *Misr Journal of Agricultural Engineering*, vol. 35, no. 1, pp. 259-274. DOI: https://doi.org/10.21608/mjae.2018.96055

[20] Yu Z. (2024). *Research and application of industrial image anomaly detection model based on deep learning (基于深度学习的工业图像异常检测模型研究与应用)*, MSc dissertation, Xi'an University of Architecture and Technology. DOI: https://doi.org/10.27393/d.cnki.gxazu.2024.001092

[21] Zhang H., Qi S., Yang R., Pan Z., Guo X., Wang W., Liu S., Liu Z., Mu J., Geng B. (2024). Design and experimentation of a potato planter missed and repeated planting detection system based on yolov7-tiny model. *INMATEH--Agricultural Engineering*, vol. 72, pp. 106-116. DOI: https://doi.org/10.35633/inmateh-72-10

[22] Zhou S., Cheng M., Xu X., Cao X. (2025). Research status and advances in perception monitoring and quality control technology for intelligent rubber roll huskers (智能胶辊砻谷机感知监测与品质调控技术研究现状及进展). Food & Machinery, vol. 41, no. 05, pp. 241-248. DOI: https://doi.org/10.13652/j.spjx.1003.5788.2024.80979

[23] Zhu Z. (1979). Preliminary study on severe rubber roll eccentricity and intense machine vibration in cantilever counterweighted rubber roll huskers (关于悬臂式重铊紧辊胶辊砻谷机的胶辊严重失圆及机体强烈振动问题的初步探讨). *Grain Industry*, no. 4, pp. 25-37.

[24] Zhu Z., Wang Y., Wang D., Yang G., Xie Z. (2024). Evaluation of array capacitive sensor for local concentration measurement of gas–solid particles flow by coupled fields based on CFD-DEM. *Measurement*, vol. 229, pp. 114457. DOI: https://doi.org/10.1016/j.measurement.2024.114457